International Journal of Engineering & Technology, 7 (4.40) (2018) 66-69

International Journal of Engineering & Technology

Website: www.sciencepubco.com/index.php/IJET

Research paper

Design and Performance of Swirl Flow Microbubble Generator

Hilman Syaeful Alam[1]*, Grace Gita Redhyka[2], Bahrudin[3], Anto Tri Sugiarto[4], Taufik Ibnu Salim and Inda Robbihi Mardhiya[6]

[1,2,3,4,5]*Technical Implementation Unit for Instrumentation Development, Indonesian Institute of Sciences, Jl. Sangkuriang Komplek LIPI Gedung 30 Bandung, 40135, Indonesia.*
[2]*Division of Frontier Materials Science, Graduate School of Engineering Science, Osaka University.*
[6]*Physics Departement, Faculty of Mathematics and Natural Science, University of Lampung, Jl. Prof. Dr. Sumantri Brojonegoro No. 1, Bandar Lampung, 35145, Indonesia.*
**Corresponding author E-mail: hilm003@lipi.go.id*

Abstract

The design of a microbubble generator that has high efficiency and good performance is still a challenge today, especially for a large scale application. In this study, CFD simulation based on the transient operation was used to predict the characteristics of a fluid flow as a reference in the design process. To analyze the performance of the swirl flow microbubble generator, particle image velocimetry (PIV) was used to characterize the dimension and distribution of microbubbles. Based on the simulation results, CFD was able to visualize the mixing process and the fluid characteristics of the gas-liquid flow in a swirl flow microbubble generator. Air self-suction mechanism in a microbubble generator nozzle was successfully formed by a negative pressure in the central axis area of the nozzle due to a swirl flow of water. It shows that a swirl flow microbubble generator can work efficiently and doesn't need any other devices to deliver air into the system. Based on the PIV measurement, the microbubbles were successfully formed with the radius averaged of 25 µm for both air mass flow rate of 0.25 l/min and 1 l/min. However, the smaller the mass flow rate of air, the more the number of microbubbles generated.

Keywords: *CFD, microbubble, unsteady, swirl flow, particle image velocimetry.*

1. Introduction

Since the last few years, microbubble technology has become an issue that attracts many researchers, because it has wide applications in various fields of science and technology, e.g. floatation and separation processes in mineral processing industry [1], oil-in-water separation in oily wastewater treatment [2], separation in plastic recycling industry [3], pre-treatment process in palm oil mill treatment system [4], aeration of cell culture in stirred bioreactors [5], increasing dissolved oxygen in fish farm [6], growth promotion of living plants, fishes, and mice [7], and so on. Microbubble has unique physical properties such as its ability to be more stable in the liquid than the ordinary bubble and it has high levels of gas solubility in liquids. Microbubble is defined by the size of the diameter of the bubble which has a bubble diameter size between 10 and 50 µm [8]. There are several methods for generating microbubbles. Zipperian [9] uses a gas injection passed on a fine porous material, then reduces the pressure of the pressurized fluid rapidly resulting in shear forces that produce microbubbles. In this system, it is very difficult to produce a bubble size with a fine size because the air bubbles will be pressurized and potentially will expand so that the size of the bubble will be enlarged due to surface tensile at the time of the injection process and then require a large energy to inject air through a fine porous material. Iwaki et al. [10] use a porous rotating device in which air is inserted into water through the rotator to produce a cavitation due to shear force from the high rotation. However, this system will cause a large energy consumption to rotate the rotator with high rpm and require high operating and maintenance costs. Then, it will cause a problem if applied in the field of fisheries or the like, because it can injure or make fish die.

The swirl flow microbubble generator is one of the efficient microbubble generating devices which potentially applied for industrial scales in the large area applications. A swirl flow microbubble generator consists of a cylindrical or conical part that will create a swirling liquid flow due to a pressurized water. Therefore, it will cause a negative pressure in the central axis of the cylindrical or conical part. The gas will be automatically inhaled to the cylinder due to the negative pressure and the centrifugal force which are generated the fine bubbles due to high smashed and shears of the fluids at the outlet of the cylinder. Ohnari [11] developed a swirl flow microbubble generator that produced microbubbles with a diameter of not more than 20 µm for industrial scale. Takase and Tsutsumi [12] developed the dual-chamber swirl flow microbubble generator which has a simple configuration and portability. However, the design of a microbubble generator that has high efficiency and good performance is still a challenge today, especially for a large scale application. In recent years, many types of research are carried out experimentally that require huge costs and time, and very few reports that study the characteristics of multiphase flow for the applications of microbubble generation. The rapid development of computational methods has allowed the design process based on virtual prototyping technique which uses a numerical simulation to explore a mixing process of the two-phase flow in microbubble generator. The numerical method based on computational fluid dynamic (CFD) simulation has been used and can be solved the problems of multiphase flow for several applications in the industry, such as: multiphase scroll pump

[13], pump-mix mixer [14], self-priming pump [15], liquid–gas jet pumps [16], and others.

2. Methods

In this study, CFD simulation was employed to characterize the gas-liquid flow in a swirl flow microbubble generator based on the unsteady multiphase flow problem. To analyze the performance of the swirl flow microbubble generator, particle image velocimetry (PIV) was used to characterize the dimension and distribution of microbubbles experimentally based on the image processing methods.

2.1. A mathematical model for CFD simulation

According to Huang et al. [15], there are two modeling techniques of multiphase flows analysis that particular uses for CFD simulation i.e. Lagrangian and Eulerian. The latter technique is able to simulate multiphase flows with a wide range of volume fraction which each phase is treated as interpenetrating continua. In this research, the multiphase flows problem was investigated as turbulently gas-liquid flow. Therefore, the Reynolds Average Navier-Stokes (RANS) equation was chosen for modeling turbulence and mixing process of gas-liquid flow in microbubble generator. In this case, the conservation equation for multiphase flow is based on the following equations [15][17]:

Continuity equation:

$$\frac{\partial \alpha_q}{\partial t} + \nabla \cdot \left(\alpha_q \vec{v}_q\right) = 0 \tag{1}$$

Momentum Equations:

$$\frac{\partial}{\partial t}\left(\alpha_q \rho_q \vec{v}_q\right) + \nabla \cdot \left(\alpha_q \rho_q \vec{v}_q \vec{v}_q\right) = -\alpha_q \nabla p + \nabla \cdot \left[\tau_q\right] + \alpha_q \rho_q \vec{g} + \alpha_q \rho_q \left(+\vec{F}_{lift,q} + \vec{F}_{vm,q}\right) + \sum_{p=1}^{n} K_{pq}\left(\vec{v}_p - \vec{v}_q\right) \tag{2}$$

Phase stress-strain tensor:

$$\left[\bar{\tau}_q\right] = \alpha_q \mu_q \left(\nabla \vec{v}_q + \nabla \vec{v}_q^{\,T}\right) + \alpha_q \left(\lambda_q - \frac{2}{3}\mu_q\right) \nabla \cdot \vec{v}_q [I] \tag{3}$$

Reynolds stress tensor:

$$\tau_q' = -\frac{2}{3}\left(\rho_q k_q + \rho_q \mu_{t,q} \nabla \cdot \vec{v}_q [I]\right) + \rho_q \mu_{t,q} \left(\nabla \vec{v}_q + \nabla \vec{v}_q^{\,T}\right) \tag{4}$$

Turbulent viscosity:

$$\mu_{t,q} = \rho_q C_\mu \frac{k_q^2}{\varepsilon_q} \tag{5}$$

Turbulent kinetic energy k_q:

$$\frac{\partial}{\partial t}\left(\alpha_q \rho_q k_q\right) + \nabla \cdot \left(\alpha_q \rho_q \vec{v}_q k_q\right) = \nabla \cdot \left(\alpha_q \frac{\mu_{t,q}}{\sigma_k} \nabla k_q\right) + \left(\alpha_q G_{k,q} - \alpha_q \rho_q \varepsilon_q\right) + \sum_{l=1}^{N} K_{lq}\left(C_{lq} k_l - C_{ql} k_q\right) - \sum_{l=1}^{N} K_{lq}\left(\vec{v}_l - \vec{v}_q\right) \frac{\mu_{t,l}}{\sigma_l} \nabla \alpha_l + \sum_{l=1}^{N} K_{lq}\left(\vec{v}_l - \vec{v}_q\right) \frac{\mu_{t,q}}{\sigma_q} \nabla \alpha_q \tag{6}$$

Turbulent dissipation ratio ε_q:

$$\frac{\partial}{\partial t}\left(\alpha_q \rho_q \varepsilon_q\right) + \nabla \cdot \left(\alpha_q \rho_q \vec{v}_q \varepsilon_q\right) = \nabla \cdot \left(\alpha_q \frac{\mu_{t,q}}{\sigma_\varepsilon} \nabla \varepsilon_q\right) + \frac{\varepsilon_q}{k_q}\left[C_{1\varepsilon} \alpha_q G_{kq} - C_{2\varepsilon} \alpha_q \rho_q \varepsilon_q + C_{3\varepsilon}\left(\sum_{l=1}^{N} K_{lq}\left(C_{lq} k_l - C_{ql} k_q\right) - \sum_{l=1}^{N} K_{lq}\left(\vec{v}_l - \vec{v}_q\right) \frac{\mu_{t,l}}{\sigma_l} \nabla \alpha_l + \sum_{l=1}^{N} K_{lq}\left(\vec{v}_l - \vec{v}_q\right) \frac{\mu_{t,q}}{\sigma_q} \nabla \alpha_q\right)\right] \tag{7}$$

where α_q is volume fraction of phase qth, λ_q and μ_q are bulk viscosity and shear one. $\vec{g}$ is acceleration due to gravity. K_{pq} is the coefficient of momentum exchange term for turbulent flows. $\vec{F}_{lift,q}$, $\vec{F}_{vm,q}$, $\vec{F}_q$ are the lift force, external body force and virtual mass force, respectively.

2.2. 3D Design & CFD simulation

Design of swirl flow microbubble generator is firstly inspired by Hato [18]. In this research, a swirl flow microbubble generator was designed by two cylindrical chambers i.e. the inner and outer chamber, as shown in Fig. 1(a). The shape of the outer chamber was designed having the circumferential inlet which leads the liquid flowed in the circumferential direction to generate a swirl flow of fluid in the inner chamber. It would cause a negative pressure in the central axis of the inner chamber and the gas would be automatically inhaled into the inner chamber. In geometric modeling, ANSYS Design Modeler was employed to build a 3D model of swirl flow microbubble generator. The computational domains based on 3D model consisted of solid and fluid domains were built using ANSYS CFX and the latter tool was also used for mesh generation and CFD simulation. Tetrahedral elements option was chosen in the meshing of the fluid domain to adjust to the complex geometry of each part as shown in Fig. 2(b). The results of mesh generation of the fluid domain produced 75,765 elements and 15,539 nodes.

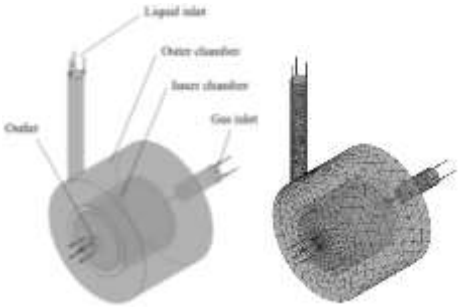

(a) (b)

Fig. 1: (a) 3-D computational domains, (b) mesh generation for the fluid domain.

2.3. Boundary conditions

Before running the CFD simulation in ANSYS CFX, we firstly must set up the boundary condition. The transient simulation was chosen as an analysis type with the total time of 5 s and time steps of 0.05 s. In liquid inlet section, the inlet mass flow rate of the liquid was set respectively 50 l/min in accordance with the design conditions. In the gas inlet section, the air inlet pressure was set at 1.0 atm, because the microbubble generator was designed to be self-suction of gas. Also, the pressure at the outlet section was set at 1.0 atm because the head pressure was below 1 m. In the governing equations according to section 2.1, the standard k-ε turbulence models for the two-phase flow simulation was chosen using the second-order upwind discrete scheme, the turbulence kinetic energy, and the turbulent dissipation ratio. While the heat transfer process was assumed as the homogeneous model and isothermal.

2.3. PIV Measurement

According to Ziegenhein et al. [19], microbubbles can be identified by using particle image velocimetry. This technique used microbubbles as particle tracers which are simple and inexpensive methods for reliable measurements in the multi-phase flow, therefore, microbubbles are possible to be characterized using PIV. In this study, microbubbles were detected by using particle image velocimetry (PIV). The PIV device arrangement consists of a digital camera, a laser diode with optical settings and a container which are shown in Fig.2.

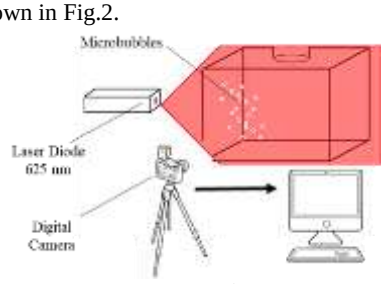

Fig. 2: Experimental setup of PIV measurement.

The steps of microbubbles characterization based on PIV measurement which are shown in Fig. 3, consist of bubble generation, video recording of rising bubble movement, image sequence extraction, particle (bubble) displacement calibration (pixels to micrometers), particle displacements to velocity measurements, particle size estimation and bubble size distribution. The measurement process was carried out using a window size of 16x16 pixels interrogation. The series of matrix values obtained from the pairing image was the distance of microbubble displacement in pixel form. While the time used was the number of images per second when the recording was 25 fps (frame per second). Based on the equation in Stokes' Law used to obtain the radius of microbubble [19]:

$$V = \frac{2}{3}\frac{\rho_f - \rho_g}{\mu} g R^2 \quad (8)$$

with V is the bubble rising velocity of the surface, ρ_f is the water density, ρ_g is the air density, μ is the viscosity of the fluid, g is the acceleration of gravity and R is the bubble radius. According to Hato [18], the smaller the amount of mass flow rate, the smaller the size of microbubble and the greater the microbubble produced, therefore the experimental investigation using PIV was conducted in two conditions, i.e. mass flow gas of 0.25 l/min and 1 l/min to investigate the effect of mass flow gas on microbubble production.

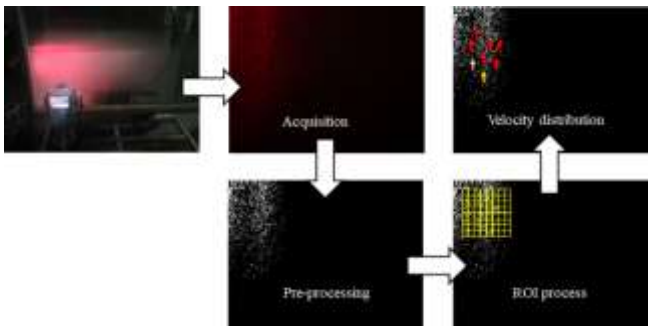

Fig. 3: The microbubbles characterization based on PIV measurement.

3. Results & Discussions

3.1. Distribution of two-phase flow

Fig. 4 shows the contours of gas-liquid flow on the swirl flow microbubble generator in (a) 0.5 s, (b) 1.0 s, (c) 1.5 s, and (d) 2 s. The air volume fraction during the mixing process is described by the void fraction, in which α = 1 means pure gas and α = 0 means pure liquid. Gas in the suction pipe seems inhaled to the inner chamber at 0.5 s, because of a negative pressure in the central axis area due to swirling flow of liquid and starts exhausted from the outlet of the chamber at 1.0 s. It is indicated that the swirl flow microbubble generator is succeeded in working with self-suction mechanisms. Almost 30% of gas starts inhaled to the inner chamber at 1.5 s and it is concentrated along the inner chamber and almost uniform from a suction pipe to the outlet at 2.0 s. It shows that a swirl flow microbubble generator works well on mixing the gas and liquid.

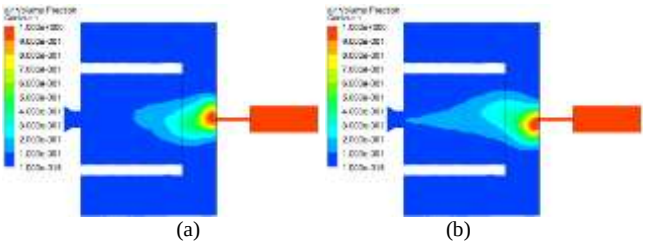

(a) (b)

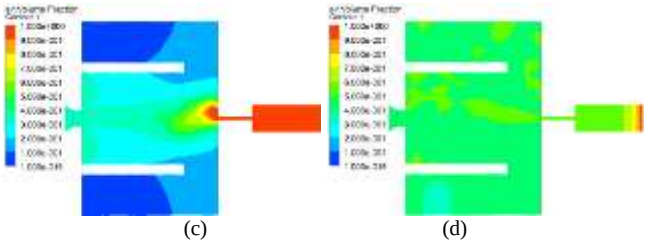

(c) (d)

Fig. 4: Gas-liquid two-phase contours on vertical planes (a) t = 0.5 s, (b) t = 1.0 s, (c) t = 1.5 s, and (d) t = 2.0 s.

3.2. Gas-liquid flow field

Fig. 6 (a) and (b) show the velocity vector of water and air at the time of 2 s. It shows that a swirl flow pattern is formed in the circumferential direction of the inner chamber due to the geometry of the liquid inlet. It will cause the negative pressure at the central axis of the inner chamber and the atmospheric gas will start to enter into the chamber. At this moment, the air superficial velocity reaches a maximum of 28.02 m/s which is approximately two times higher than the water superficial velocity of 11.11 m/s, because there is a difference of density between two fluids. The fluid velocity in both the outer and inner chamber is lower than the outlet of the system because the kinetic energy is converted into the pressure energy.

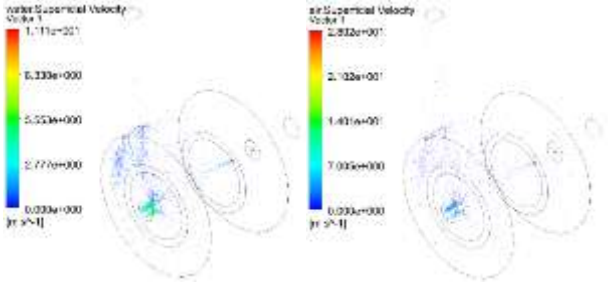

(a) (b)

Fig. 5: Vectors of the superficial velocity for (a) water and (b) air at t = 2.0 s.

3.3. Distribution of the pressure fields

Fig. 6 (a) and (b) shows the pressure distribution of the swirl flow microbubble generator in 0.5 s and 1.5 s respectively. From both images, the pressure at the central axis of the inner chamber is gradually decreased in line with the increasing of time until it is in a state of vacuum at t =1.5 s. Therefore, the gas will be inhaled into the chamber by the self-suction mechanism. By a high speed and pressure, the fine gas bubbles will be generated due to high smashes and shears of the fluids at the outlet of the chamber. However, if we compare with former research [17], the swirl flow type is more efficient than the dual chamber types, because the negative pressure generated in the system is slightly higher, so the gas-liquid ratio can increase in the same boundary conditions.

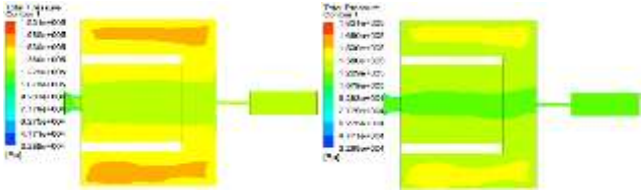

(a) (b)

Fig. 6: Pressure distribution on a vertical plane, (a) 0.5 s, and (b) 1.5 s.

3.4. Measurement results of PIV

The measurement results of PIV in the form of a video converted into an extracted sequence of images resulted in a 3-dimensional matrix. The size and distribution of microbubble using PIV are calculated based on the image pair matrix with an air mass flow rate of 0.5 l/min and 1 l/min respectively using a window size of

16x16 pixels interrogation. In the image processing with an air mass flow rate of 1 l/min produces 5,652 images and at an air mass flow rate of 0.25 l/min produces 5,232 images. Fig. 7 shows the bubble distribution and size of the 99-107 image pair matrix at the air flow rate (a) 1 l/min and (b) 0.25 l/min. The size of bubble radius both in the air mass flow rate of 1 l/min and 0.25 l/min average about 25 µm, but the number of microbubbles in the air mass flow rate of 0.25 l/min is higher than those of 1 l/min. This is in accordance with the results obtained by Hato et al. [18], where the smaller the mass flow rate gas, the smaller the size and the more the number of microbubbles generated.

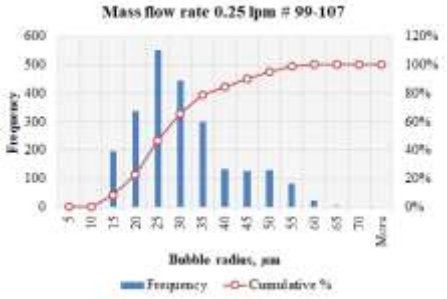

(a)

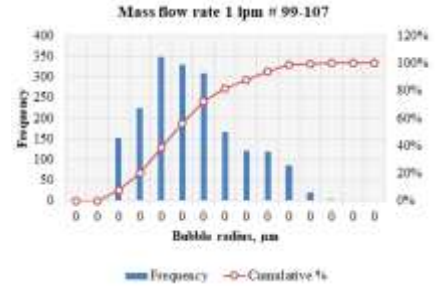

(b)

Fig. 7: The distribution and size of microbubbles in the image-pair matrix 99-107 at air flow rate (a) 1 l/min and (b) 0.25 l/min.

4. Conclusion

Design and development a swirl flow microbubble generator using CFD simulation is able to visualize the mixing process and the fluid characteristics of the gas-liquid flow in a swirl flow microbubble generator. The swirl flow microbubble generator is able to dissolve a gas into the liquid by a self-suction mechanism. It means that a swirl flow microbubble generator doesn't need any other devices to deliver air into the system. The fluid velocity in both the outer and inner chamber is lower than the outlet of the system because the kinetic energy is converted into the pressure energy. The air superficial velocity is two times higher than water superficial velocity because there is a difference of density between two fluids. By a high speed and pressure, the fine gas bubbles will be generated due to high smashes and shears of the fluids at the outlet of the chamber. Based on the experiment, a swirl flow microbubble generator able to generate the fine bubbles. The size of microbubbles from PIV measurement results for both the air mass flow rate of 1 l/min and 0.25 l/min was an average of 25 µm and could be categorized as fine bubbles. However, the number of microbubbles in the air mass flow rate of 0.25 l/min was higher than those of the air mass flow rate of 1 l/min. Therefore, the smaller the mass flow rate of air, the more the number of microbubbles generated.

Acknowledgment

This work was financed by Kegiatan Prioritas Nasional (PN) 2018, Indonesian Institute of Sciences (LIPI). The author would like to thank the Head of Research Center for Electrical Power and Mechatronics, Indonesian Institute of Sciences, for facilitating the CFD simulation using ANSYS.

References

[1] S. Calgaroto, A. Azevedo, and J. Rubio, "Flotation of quartz particles assisted by nanobubbles," Int. J. Miner. Process., vol. 137, pp. 64–70, 2015.

[2] X. Li, H. Xu, J. Liu, J. Zhang, J. Li, and Z. Gui, "Cyclonic state micro-bubble flotation column in oil-in-water emulsion separation," Sep. Purif. Technol., vol. 165, pp. 101–106, 2016.

[3] P. Basařová, T. Váchová, G. Moore, G. Nannetti, and J. Pišlová, "Bubble adhesion onto the hydrophobic surface in solutions of non-ionic surface-active agents," Colloids Surfaces A Physicochem. Eng. Asp., vol. 505, pp. 64–71, 2016.

[4] S. Tabassum, Y. Zhang, and Z. Zhang, "An integrated method for palm oil mill effluent (POME) treatment for achieving zero liquid discharge - A pilot study," J. Clean. Prod., vol. 95, pp. 148–155, 2015.

[5] D. Druzinec, D. Salzig, M. Kraume, and P. Czermak, "Micro-bubble aeration in turbulent stirred bioreactors: Coalescence behavior in Pluronic F68 containing cell culture media," Chem. Eng. Sci., vol. 126, pp. 160–168, 2015.

[6] A. Endo et al., "DO-increasing effects of a microscopic bubble generating system in a fish farm," Mar. Pollut. Bull., vol. 57, no. 1–5, pp. 78–85, 2008.

[7] K. Ebina et al., "Oxygen and Air Nanobubble Water Solution Promote the Growth of Plants, Fishes, and Mice," PLoS One, vol. 8, no. 6, pp. 2–8, 2013.

[8] A. Agarwal, W. J. Ng, and Y. Liu, "Principle and applications of microbubble and nanobubble technology for water treatment," Chemosphere, vol. 84, no. 9, pp. 1175–1180, 2011.

[9] D. E. Zipperian, "Method and apparatus for generating microbubbles in froth flotation mineral concentration systems." European Patent Applications, Publication Number: 0364654A2, Date of Patent: Feb. 22, 1989.

[10] C. Iwaki, K. Aoki, H. Komita, "Microbubble Generating Apparatus And Method," United States Patent, Patent No.: US 8,678,356 B2, Date of Patent : Mar. 25, 2014.

[11] H. Ohnari, "Swirling Type Micro-Bubble Generating System," United States Patent, Patent No.: US 7,472,893 B2, Date of Patent: Jan. 6, 2009.

[12] Takase and H. Tsutsumi, "Microbubble Generating Apparatus," United States Patent, Patent No.: US 8,939,436 B2, Date of Patent: Jan. 27, 2015.

[13] J. Wang, H. Zha, J. M. McDonough, and D. Zhang, "Analysis and numerical simulation of a novel gas-liquid multiphase scroll pump," Int. J. Heat Mass Transf., vol. 91, pp. 27–36, 2015.

[14] Y. Zou, S. Ye, Y. Wang, and W. Fei, "CFD simulation and PIV measurement of liquid-liquid two-phase flow in pump-mix mixer," J. Taiwan Inst. Chem. Eng., vol. 60, pp. 15–25, 2016.

[15] S. Huang, X. Su, J. Guo, and L. Yue, "Unsteady numerical simulation for gas-liquid two-phase flow in self-priming process of a centrifugal pump," Energy Convers. Manag., vol. 85, pp. 694–700, 2014.

[16] G. Yuan, L. Zhang, H. Zhang, and Z. Wang, "Numerical and experimental investigation of the performance of the liquid – gas and liquid jet pumps in desalination systems," DES, vol. 276, no. 1–3, pp. 89–95, 2011.

[17] H. S. Alam, Bahrudin, A. T. Sugiarto and G. G. Redhyka, "Unsteady numerical simulation of gas-liquid flow in dual chamber microbubble generator," 2017 2nd International Conference on Automation, Cognitive Science, Optics, Micro Electro--Mechanical System, and Information Technology (ICACOMIT), Jakarta, 2017, pp. 133-137. doi: 10.1109/ICACOMIT.2017.8253401

[18] Y. Hato, " Micro-Bubble Generator And Micro-Bubble Generation Device," United States Patent, Patent No.: US 2012/0126436 A1, Date of Patent: May 24, 2012.

[19] T. Ziegenhein, M. Garcon, and D. Lucas, "Particle tracking using microbubbles in bubbly flows," Chem. Eng. Sci., vol. 153, pp. 155–164, 2016.